Computer Fraud and Security
ISSN (online): 1873-7056

Integrated Control Strategy of Variable Coefficient Virtual Inertia for Doubly-Fed Wind Turbines with Primary Frequency Regulation

YU Da[1], WANG YanYue[2,*], YAN YuXin[2], LIN Xu[1], WANG WeiHua[1]

1. Department of Grid Connection and New Energy Management, Electric Power Dispatching Control Center of Guangdong Power Grid Co., Ltd., Guangzhou 510030, China;

2. College of Electrical and Electronic Engineering, State Key Laboratory of Alternate Electrical Power System with Renewable Energy Sources(North China Electric Power University), Beijing 102206, China

Email: dale_yuda@163.com

Email: 2549533327@qq.com

Project supported by China Southern Power Grid Corporation Science and Technology Project Funding Project (Grant No. GDKJXM20220335)

Abstract: Wind power generation has emerged as one of the most scalable renewable energy sources. However, the decoupling of wind turbine speed from grid frequency in doubly-fed induction generators (DFIGs) while tracking maximum power leads to a lack of frequency regulation capability in wind power systems. To address this issue, a comprehensive control strategy is proposed, integrating the variable virtual inertia control of DFIGs with primary frequency control, enabling the wind turbines to achieve comprehensive control over system frequency and smooth out frequency fluctuations. This control mechanism employs a dynamic factor based on frequency deviation, allowing for a rapid increase in electromagnetic power during significant frequency drops, effectively supporting grid frequency. Through an in-depth analysis of the primary frequency control capabilities of wind turbines, the pitch angle control has been improved, resulting in a control strategy that allows for flexible adjustment of the static regulation coefficient of wind turbines. Simulation results validate the feasibility of the proposed frequency control strategy.

Keywords: doubly-fed induction generator (DFIG); maximum power point tracking; virtual inertia control; primary frequency regulation; pitch angle

Introduction

Doubly Fed Induction Generators (DFIGs) [1], as the dominant technology in large-scale wind farms, achieving maximum power point tracking (MPPT) [2] by independent control of active and reactive power, thereby enhancing wind energy utilization. However, their decoupled control between rotor speed and grid frequency inherently restricts the utilization of rotor kinetic energy for primary frequency response (PFR), presenting significant challenges to modern power systems.

With the continuous growth in renewable energy penetration[3], the decline in system inertia has weakened grid PFR capability. Traditional wind turbines operate passively in frequency-agnostic mode, solely relying on mechanical inertia to mitigate frequency deviations without actively contributing. Consequently, there is an urgent need to develop frequency control strategies for modern power systems with high wind penetration, accelerating the transition of wind turbines from being un-supported and passively resisting disturbances to proactive frequency support. By employing supplementary control mechanisms that fully utilize rotor kinetic energy for frequency regulation, this research aims to achieve precise frequency response to load variations and enhance the overall frequency regulation capability of wind farms.

Extensive research has been conducted globally to enable wind turbines to actively participate in system frequency regulation, with two main technical pathways emerging:

1) Inertia control[4], including virtual inertia control (VIC) [5] and droop control[6]. Virtual inertia control adds an additional control module based on rate of change of frequency (ROCOF) to emulate synchronous machine inertia characteristics[7], thereby increasing active power output for frequency support. Literature[8] proposes a comprehensive inertia control strategy based on a piecewise gain-scheduled approach, demonstrating effective frequency regulation capability for wind turbines operating below rated wind speed. Literature [9] proposes a variable-coefficient inertia control method that improves frequency regulation performance under large disturbances, allowing the rotor speed to smoothly return to MPPT after exiting frequency support mode. Droop control[10] adjusts additional active power generation through proportional gain of frequency deviation, mimicking synchronous machine damping response. Literature[11] establishes a variable droop curve based on wind turbine active power output and system frequency, switching to a dedicated frequency regulation mode during severe frequency drops. Literature[12] sets the droop coefficients for wind turbines across low, middle and high wind speed regions, achieving stable frequency response while maintaining operational reliability. While droop control provides continuous active power support over a longer duration compared to VIC, its droop coefficient setting poses significant challenges. In summary, although inertia control responds rapidly to frequency fluctuations for immediate support, it has limitations in sustained frequency regulation under load variations. Moreover, the recovery of rotor kinetic energy during system restoration may induce secondary frequency drops.

2) Power reserve control[13] encompasses overspeed control[14], pitch angle control[15], and their hybrid implementations. Overspeed control operates the wind turbine at non-maximum power point tracking mode by increasing rotor speed, thereby reserving a certain frequency regulation margin to meet emergency active power augmentation requirements[16]. Literature[17] proposes a frequency regulation energy function that integrates ROCOF, minimum frequency point, and steady-state frequency deviation to determine optimal overspeed operation points for wind turbines. This function serves as a reference for calculating the active power augmentation required during frequency emergencies. Literature[18] quantifies the relationship between overspeed load shedding and equivalent inertia time constant, presenting a control method that adjusts WT active power output based on frequency fluctuation severity. Literature[19] determines the control parameters for overspeed load shedding based on wind turbine operating states, simultaneously utilizing both rotor kinetic energy and reserve power for frequency support. Pitch angle control modulates the mechanical power capture of wind turbines by adjusting the blade pitch angles. Smaller pitch angles lead to a greater mechanical power capture[20]. This enables the wind turbine to intentionally deviate from MPPT operation, reserving a certain amount of power capacity for frequency stabilization. Literature[21] employs wind speed forecast models to calculate frequency response time and frequency control controllability margin, enabling dynamic optimization of pitch angles. Literature[22] proposes an optimal pitch angle control strategy that minimizes the movements of the pitch actuator for determining active power adjustment commands, thus effectively reducing mechanical wear. Although power reserve control can effectively reduce frequency deviation by generating the reserved frequency regulation reserve power, its inherently slow response characteristics make it inapplicable to grids in scenarios with frequent frequency fluctuations.

It is worth noting that wind farms must possess controllable inertial response combined with primary frequency response capability to achieve comprehensive frequency regulation. The aforementioned literature has placed greater emphasis on investigating improved inertial control or enhanced power reserve control strategies for improving system frequency characteristics. However, in-depth investigations into hybrid control schemes integrating primary frequency regulation with virtual inertia control under reduced-load operation modes are still lacking.

To enhance the frequency stability of power systems with high wind penetration, this study investigates an improved virtual inertia control strategy for DFIGs. By optimizing the fixed proportionality coefficient in classical virtual inertia control and introducing a dynamic power tracking ratio coefficient, a hybrid control scheme combining virtual inertia control with PFR is proposed. This strategy enables the output power of the DFIG to vary linearly with frequency deviation, thereby effectively suppressing frequency fluctuations induced by load variations. To validate the proposed control strategy's effectiveness during system frequency disturbances, a power system simulation model comprising a wind farm cluster and three thermal power plants is established using PSCAD/EMTDC. The simulation results showcase the dynamic responses of DFIGs during frequency dips and confirm the proposed strategy's superiority in frequency support capability.

1 Mathematical Model of DFIG

1.1 DFIG Mathematical Model

Based on the principles of aerodynamics, the mechanical power P_m of a wind turbine can be expressed as[23]:

$$P_m = 0.5\rho\pi R^2 v_w^3 C_p\left(\beta,\lambda\right) \tag{1}$$

Where ρ is the air density, R is the rotor blade length, v_w is the wind speed, C_p is the wind power coefficient, β is the pitch angle, λ is the tip speed ratio.

The tip speed ratio of a wind turbine is defined as the ratio of the blade tip speed to the natural wind speed:

$$\lambda = \frac{R\omega_r}{v_w} \tag{2}$$

As can be seen from Equation (1), the mechanical power output of a wind turbine under fixed wind speed conditions is significantly affected by the power coefficient C_p. The value of C_p is determined by key parameters including the pitch angle and tip speed ratio of the wind turbine. This relationship can be mathematically described using a high-order nonlinear function[24]:

$$\begin{cases} C_p\left(\beta,\lambda\right) = c_1\left(\dfrac{c_2}{\lambda_i} - c_3\beta - c_4\right)e^{\frac{-c_5}{\lambda_i}} \\ \dfrac{1}{\lambda_i} = \dfrac{1}{\lambda + 0.08\beta} - \dfrac{0.035}{\beta^3 + 1} \end{cases} \tag{3}$$

The constant parameters c_1~c_5 in equation (3) are determined by the specific wind turbine model. The parameter values of the DFIG model in this study are listed in Table 1[25].

Table 1 Wind turbine parameters

parameters	value
c_1	0.22
c_2	116
c_3	0.4
c_4	5
c_5	12.5

According to equation (3), the relationship between the pitch angle β, tip speed ratio λ, and wind power coefficient C_p can be derived, as illustrated in Figure 1.

As shown in Figure 1, increasing the pitch angle β causes the C_p-λ curve to shrink and the peak value of C_p to decline, thus reducing the mechanical power output of the wind turbine. When β is kept constant, C_p initially increases with λ until reaching a maximum point and then decreases subsequently.

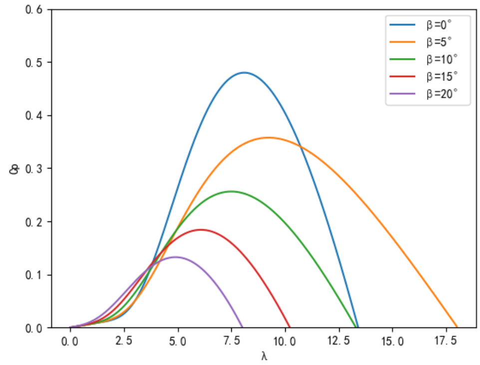

Fig. 1 C_p-λ curve corresponding to different pitch angles

When the tip speed ratio λ equals the optimal value λ_{opt} on the C_p-λ curve, the maximum power coefficient $C_{p\max}$ is attained. Variationsin the pitch angle will modify both $C_{p\max}$ and λ_{opt}. Specifically, when β=0, the $C_{p\max}$ corresponding to λ_{opt} reaches its maximum value. Under constant wind speed conditions, the mechanical power output of the wind turbine can be adjusted by either varying the rotor speed or changing the pitch angle.

1.2 Maximum Power Tracking Control

Under constant wind speed conditions, the mechanical power output of a DFIG is primarily influenced by the rotor rotational speed, as variations in it directly affect the tip speed ratio and consequently the wind power coefficient. When the pitch angle (β) is constant, the relationship between the mechanical power Pm and the rotor rotational speed ω_r of a DFIG under different wind speeds can be derived from Equations (1) and (2). From the perspective of wind turbine power output, the grid-connected operation of a DFIG can be divided into four distinct regions as shown in Figure 2[26]: startup phase, maximum power tracking region, constant rotor speed region, and constant power region. Among them, the wind speed levels follow the hierarchy：$v_7>v_6>v_5>v_4>v_3>v_2>v_1$。

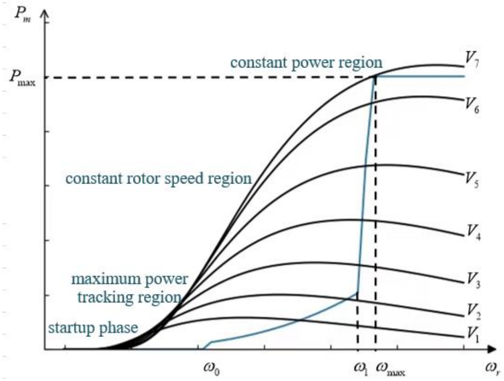

Fig. 2 Maximum power tracking point curve

To achieve maximum economic efficiency, the DFIG in a wind farm typically operates in the maximum power tracking control mode by adjusting the rotor speed and pitch angle. Maximum power tracking control entails regulating the rotor speed to maintain $\lambda=\lambda_{opt}$, enabling the DFIG to attain its maximum output power under constant wind speed conditions.

The active power reference command P_{opt}^* for the generator is provided by the feedback of the wind turbine's angular velocity ω_r[27]:

$$P_{opt}^* = \begin{cases} k_{opt}\omega_1^3, \omega_0 < \omega_r < \omega_1 \\ \dfrac{P_{\max} - k_{opt}\omega_1^3}{\omega_{\max} - \omega_1}(\omega_r - \omega_{\max}) + P_{\max}, \omega_1 < \omega_r < \omega_{\max} \\ P_{\max}, \omega_r > \omega_{\max} \end{cases} \tag{4}$$

In the equation, k_{opt} represents the coefficient of the maximum power tracking curve, ω_0 is the cut-inangular velocity of the DFIG, ω_1 is the angular velocity at which the DFIG enters the constant speed region, $\omega_{\max}$ is the maximum angular velocity of the DFIG, and $P_{\max}$ is the maximum output power of the DFIG.

When the wind turbine employs an MPPT controller, the optimal rotor speed of the wind turbine, denoted as ω_{ropt}, can be expressed as:

$$\omega_{ropt} = \frac{\lambda_{opt} v_w}{R} \tag{5}$$

Combining Equation (1), the optimal power P_{opt} obtained by the wind turbine under the MPPT controller can be derived as:

$$P_{opt} = \frac{1}{2}\rho\pi R^2 C_{p\max}\left(\frac{R}{\lambda_{opt}}\right)^3 \omega_{ropt}^3 \tag{6}$$

Then, the proportional coefficient k_{opt} of the power tracking curve is:

$$k_{opt} = \frac{1}{2}\rho\pi R^2 C_{p\max}\left(\frac{R}{\lambda_{opt}}\right)^3 \tag{7}$$

2 Comprehensive Control Strategy for Variable Coefficient Virtual Inertia Control and Primary Frequency Regulation of DFIGs

2.1 Virtual Inertia Control Strategy Based on Dynamic Power Tracking Proportional Coefficient

When a power imbalance occurs in the power system, leading to a frequency deviation, it is necessary to increase the proportional coefficient of the power tracking curve to provide frequency support and thereby enhance the electromagnetic power output of the wind turbine. Therefore, based on Equation (8), a maximum proportional coefficient $k_{\max}$ of the power tracking curve is tuned. When the wind turbine participates in frequency regulation, the optimal proportional coefficient k_{opt} of the power tracking curve is switched to the maximum proportional coefficient $k_{\max}$.

$$k_{\max} = 1/2\rho\pi R^2 C_p\left(\lambda_{opt}\right)\left(\frac{R}{\lambda'}\right)^3 \tag{8}$$

$$\lambda' = \frac{\omega_{\min} R}{v_w'} \tag{9}$$

where $\omega_{\min}$ represents the minimum rotor speed, λ' denotes the tuned tip speed ratio, v_w' represents the predicted increasing wind speed, which is tuned to 11 m/s in this study.

When the grid frequency drops, it is necessary for wind turbines to increase their output power to maintain system stability. However, continuously increasing the active power output by raising the proportional coefficient of the power tracking curve will lead to a continuous decrease in rotor speed. Therefore, after the frequency deviation decreases, it is essential to gradually adjust the proportional coefficient from the tuned maximum proportional coefficient $k_{\max}$ to the optimal proportional coefficient k_{opt}, and maintain the operation of the wind turbine along the MPPT curve until the frequency regulation is completed.

Therefore, a dynamic proportional coefficient k_v is designed, which can make the output power of the wind turbine change linearly according to the frequency deviation.

$$k_v = \left(1-\gamma\right)k_{opt} + \gamma k_{\max} \tag{10}$$

where, $$\gamma = \frac{1}{1+e^{-2n\left[\Delta f - \left(\Delta f_h - \Delta f_l\right)\right]}} \tag{11}$$

In which, γ represents the dynamic factor, n is a positive integer, Δf_l and Δf_h represent the set lower and upper limits of frequency deviation respectively.

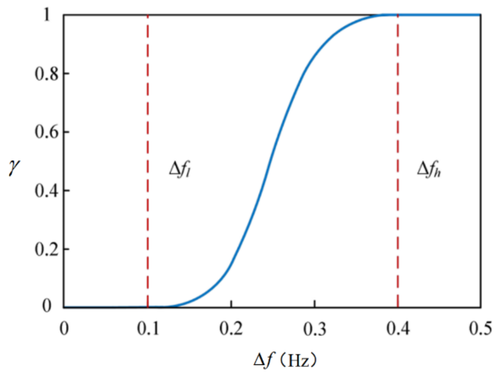

Fig. 3 Characteristics of dynamic factor γ

The characteristics of the dynamic factor γ are presented in Figure 3. By setting the frequency lower limit Δf_l and the frequency upper limit Δf_h in Equation (11), the controller can be activated when the system frequency deviation approaches Δf_l. Furthermore, the closer the frequency drop is to Δf_h, the closer the dynamic proportional coefficient k_v approaches the maximum proportional coefficient $k_{\max}$, and the greater the additional active power output of the wind turbine. When the frequency deviation decreases, the dynamic proportional coefficient k_v gradually returns to the optimal proportional coefficient k_{opt}, enabling the wind turbine to resume operation on the MPPT curve.

The setting of the dynamic proportional coefficient k_v enables the wind turbine to linearly adjust its output power according to the frequency deviation, avoiding severe jolts caused by step changes in active power. Meanwhile, it ensures that the doubly-fed wind turbine with virtual inertia control will not operate when there are slight fluctuations in the grid frequency, preventingfrequent consumption of the wind turbine rotor's kinetic energy. When the frequency drops significantly, it can act promptly to provide frequency support and maintain the frequency stability of the power system.

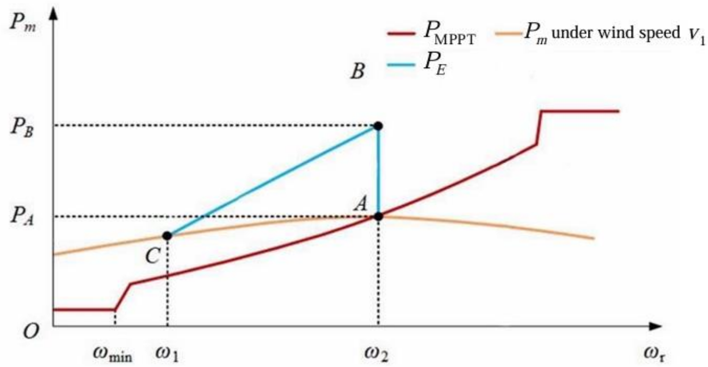

Fig. 4 Virtual inertia control strategy diagram

As can be seen from Figure 4, the frequency regulation process of the proposed virtual inertia control strategy unfolds as follows: When the wind speed is fixed at V_1, the doubly-fed wind turbine operates stably at point A under the MPPT working state[28]. In the event of a significant disturbance in the power system that causes a rapid drop in frequency, since the frequency change is relatively substantial in the early stage of the disturbance, k_{opt} will swiftly increase to $k_{\max}$, causing the electromagnetic power of the wind turbine to suddenly increase to point B. However, since the electromagnetic power output by the wind turbine is greater than the captured mechanical power, the rotor decelerates, and the operating point of the wind turbine drops along the BC curve until the wind turbine operates stably at point C. At this time, the power tracking proportional coefficient is switched back to k_{opt}, and the wind turbine rises smoothly along the curve CA to point A.

2.2 Primary Frequency Regulation Control Strategy

Primary frequency regulation[29] is an important means to achieve frequency stability in power systems.

During the process of participating in the primary frequency regulation of the power system, the DFIG can effectively take on the unbalanced power components that cause system frequency fluctuations.

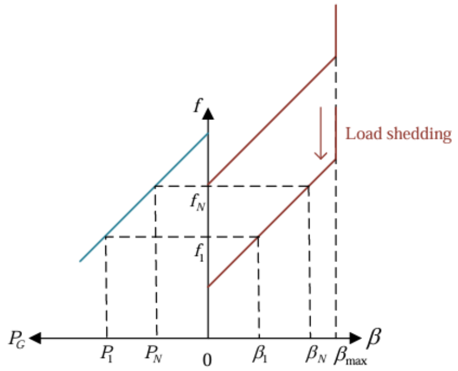

Fig. 5 The static power-frequency characteristic of wind turbine generators

As shown in Figure 5, when the system frequency is maintained at the rated frequency f_N, the corresponding output power is P_N. If the system load increases, the frequency drops to f_1. At this time, the unit can reduce the pitch angle to β_1 to increase the captured wind energy, and the mechanical power continuously increases to P_1 to participate in frequency regulation.

Similar to traditional conventional power generation equipment, define and tune the droop coefficient of the DFIG as

$$R_f = -\frac{\Delta f}{\Delta P_G} \tag{12}$$

where, ΔP_G represents the change in active power of the wind turbine when the frequency offset is Δf.

The static droop coefficient serves as the basis for the unit to share the unbalanced power during primary frequency regulation, reflecting the primary frequency regulation capability. If the value of the static droop coefficient is too small, it may lead to unreasonable load distribution among wind turbines; if the value is too large, the wind turbine faces the risk of out-of-step tripping. Therefore, the value of the static droop coefficient should be controlled within a reasonable range[30].

Doubly-fed wind turbines can participate in primary frequency regulation by adjusting the pitch angle to provide active power-frequency support to the system, similar to how conventional units participate in the primary frequency regulation of power systems. Combining Equation (12), the pitch angle-frequency characteristics of the wind turbine under normal operation and load-shedding operation can be expressed as

$$R_f = \begin{cases} -\dfrac{\beta}{\Delta P_G} R_{\beta n} \\ -\dfrac{\beta - \beta_0}{\Delta P_G} R_{\beta d} \end{cases} \tag{14}$$

In the formula, $R_{\beta n}$=$\Delta f/\beta R_{\beta d}$=$\Delta f/(\beta$-$\beta_0)$ is defined as the static pitch droop coefficient during normal operation, and $R_{\beta d}$=$\Delta f/(\beta$-$\beta_0)$ is the static pitch droop coefficient during load-shedding operation.

An integral link is introduced to achieve the setting of the static frequency characteristics of the wind turbine. The control structure block diagram is shown in Figure 6.

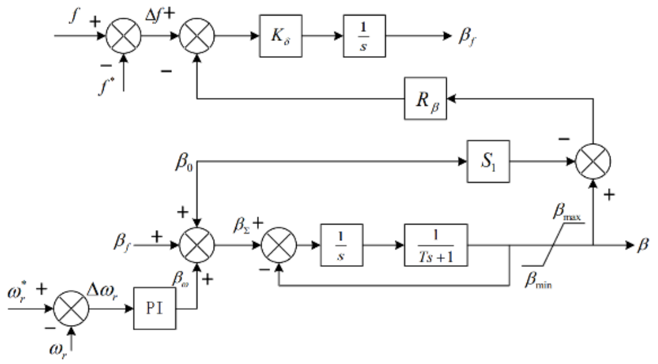

Fig. 6 Primary frequency modulation control structure diagram

In Figure 6, S_1 is the switch control command. When $S_1 = 0$, the unit does not operate in load-shedding mode; when $S_1 = 1$, the unit operates in load-shedding mode. Then the improved pitch angle control equation of the wind turbine is

$$\left\{[\Delta f - R_\beta(\beta - S_1\beta_0)]\frac{K_\delta}{s} + \beta_\omega + \beta_0 - \beta\right\}\frac{1}{s(Ts+1)} = \beta \tag{15}$$

where T is the time constant of the pitch angle servo mechanism, K_δ is the frequency gain, the DFIG enters the constant power region when the pitch angle is β_ω, β_N is the preset pitch angle of the DFIG unit during load-shedding operation.

From Equation (14), the static pitch droop coefficient of the wind turbine can be further obtained

$$R_\beta = \frac{\Delta f}{\beta - S_1\beta_0} \tag{16}$$

Firstly, the proposed control scheme conforms to the pitch angle-frequency response characteristics as shown in Equation (15). Secondly, S_1 is used to select and configure the magnitude of the static pitch droop coefficient R_β. Then, based on the actual operating conditions of the wind turbine and the reserved frequency regulation capacity, combined with Equation (13), the static droop coefficient R_f is determined. As a result, the wind turbine can effectively respond to system frequency drops or rises, thus exhibiting power-frequency static characteristics similar to those of conventional generating units.

2.3 Comprehensive Frequency Control Strategy

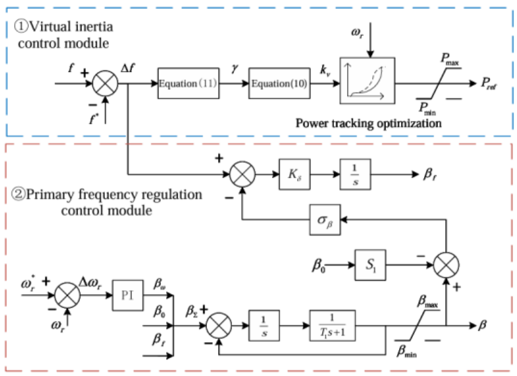

Fig. 7 Structure diagram of frequency modulation cooperative control strategy for wind farm

The frequency regulation coordination strategy proposed in this paper consists of two modules, and its structure is shown in Figure 7:

① Virtual inertia control module: By designing the dynamic power tracking proportional coefficient, the linear adjustment of the DFIG output power is achieved, thus realizing a controllable inertia response effect and effectively supporting the system frequency.

② Primary frequency regulation control module: The pitch static droop coefficients during normal operation and load-shedding operation are utilized to adjust the pitch angle, thereby setting the static droop coefficient $R\sigma_f$ of the wind turbine, and sharing the unbalanced power of the system.

During the process of wind turbine participation in frequency regulation, the key factor leading to its instability is that the system frequency drop will cause an increase in active power output, resulting in the wind turbine speed dropping below the cut-in wind speed and thus causing a shutdown failure. To address this issue, in the primary frequency regulation control strategy, gradually reducing the pitch angle can effectively increase the operating point of the wind turbine and avoid the risk of too low a speed. Accordingly, the coordinated action of the primary frequency regulation control and variable coefficient virtual inertia control proposed in this paper can significantly improve the primary frequency regulation capability and frequency response characteristics of the wind turbine.

3 Case Analysis

In order to verify the feasibility of the frequency support control strategy proposed in this paper, a power system simulation model as shown in Figure 8 is established in PSCAD/EMTDC. This simulation model includes a wind farm cluster and three thermal power generating units.

Among them, the installed capacities of the thermal power generating units G2, G3 and G4 are all 100 MW. The rated power of a single wind turbine in the wind farm is 2 MW, and there are a total of 100 wind turbines in the wind farm cluster. The rated wind speed of the wind farm is taken as 11 m/s.

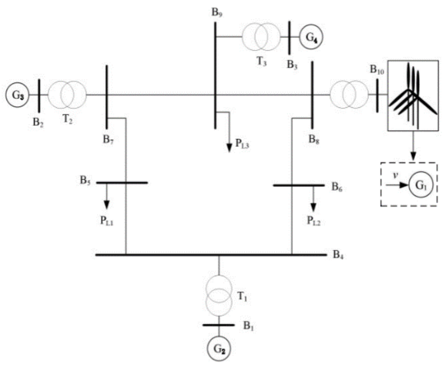

Fig. 8 Simulation model

3.1 Comparison of Frequency Regulation Effects under Sudden Load Increase

The total system load of the simulation model in this paper is 300 MW. An additional disturbance is set at the system load P_{L1}. At 15 s, an additional 50 MW is added, causing the system frequency to decrease. During the control process, the tip-speed ratio is set as λ=4.55 and the static pitch droop coefficient is set as σ_β=0.026. The proposed control strategy is compared with the cases where the wind turbine does not participate in frequency regulation and uses virtual inertia control. The simulation parameter values of the wind turbine are listed in Table 2, and the simulation results are shown in Figure 9.

Table 2 Wind turbine parameters

Parameters	Value
Rated wind speed v_N	10m/s
Rated power P_N	2MW
Blade length R	49m
Air density ρ	1.225kg/m^3
Inertia time constant H_g	4.32s
Damping coefficient D_g	0.01N·m·s/rad

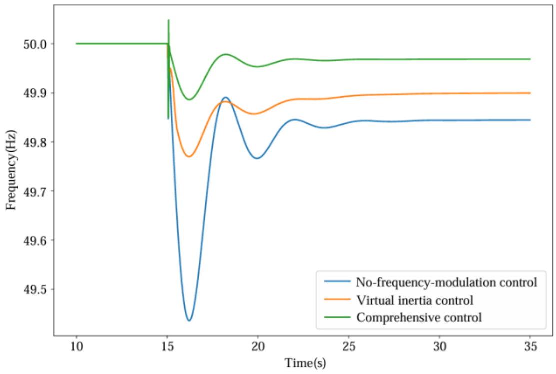

Fig. 9 System frequency change waveform after load suddenly increase 50MW

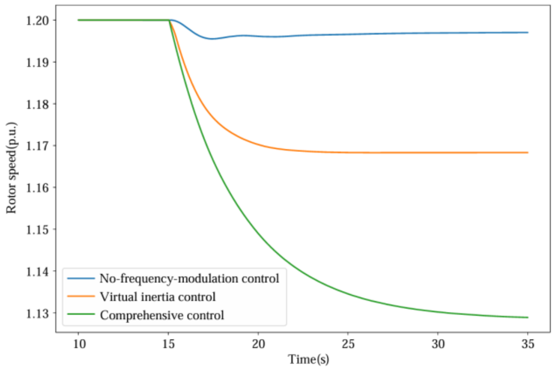

Fig. 10 System rotor speed change waveform after load suddenly increase 50MW

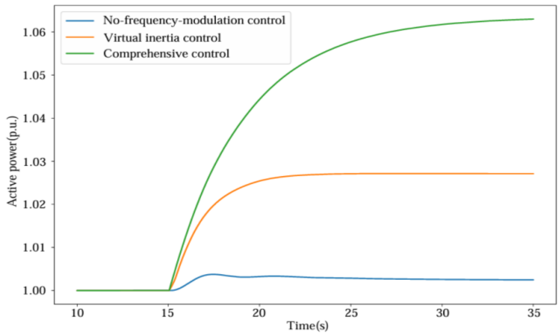

Fig. 11 Active power output change waveform after load suddenly increase 50MW

The simulation results are shown in Figures 9, 10, and 11, which respectively represent the dynamic responses of the system frequency f, the wind turbine rotational speed ω_r, and the active power output P_g of the wind turbine under three scenarios: without auxiliary frequency regulation control, with traditional virtual inertia control, and with the comprehensive frequency regulation control proposed in this paper. Through the analysis of Figures 9 - 11, it can be seen that when the system load suddenly increases and the system frequency drops, without any control applied, the response of the DFIG to the system frequency change is very weak. After introducing the traditional virtual inertia control, although the rate of change of the system frequency is reduced, the improvement effect is not significant. The wind farm frequency regulation coordination control strategy proposed in this paper can quickly increase the active power generation for frequency support, with a high response speed. The lowest point of the system frequency rises from 49.44 Hz to 49.85 Hz, and the drop amplitude is reduced by 73.2%. Moreover, in this process, the rotational speed of the wind turbine decreases, thus releasing kinetic energy and providing an effective inertia support for the system. The effect is significantly better than that of virtual inertia control.

Table 3 Frequency response

	The lowest point of the frequency (Hz)	Steady-state frequency (Hz)
No frequency regulation control	49.44	49.84
Virtual inertia control	49.77	49.90
Comprehensive control	49.85	49.97

3.2 Comparison of Frequency Regulation Effects under Continuous Disturbances with Random Wind Speeds

To further verify the effectiveness of the proposed strategy in actual operation, a white noise sequence is used to simulate random wind speeds, as shown in Figure 12.

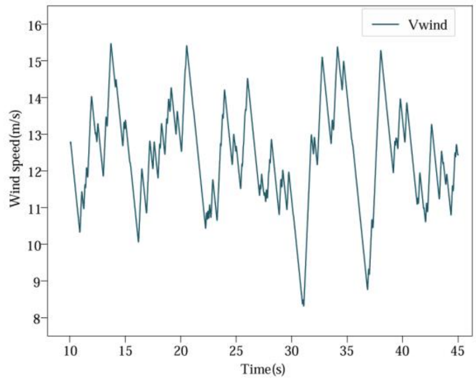

Fig. 12 Random wind speed

Set the system load to suddenly increase by 50 MW at 15 s and then increase by another 25 MW at 25 s to verify the effectiveness of the comprehensive control strategy proposed in this paper under continuous disturbances. The simulation results are shown in Figures 13, 14, and 15.

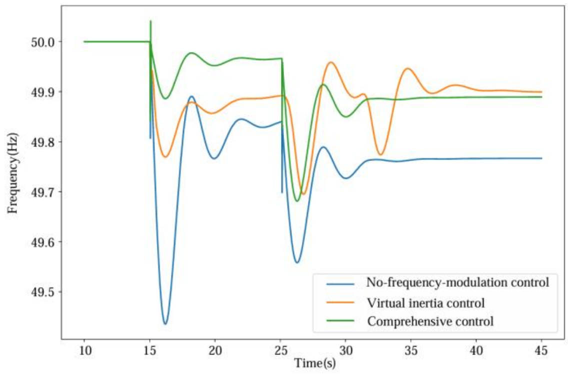

Fig. 13 Frequency variation waveform under continuous disturbance

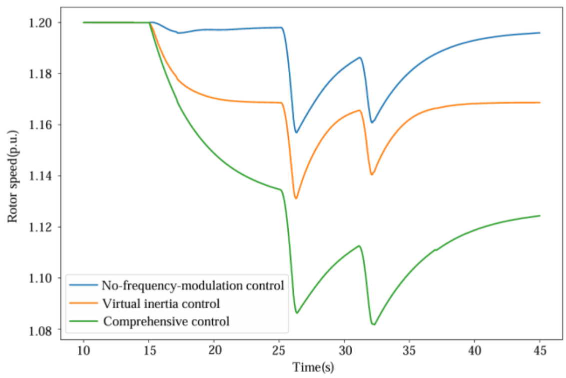

Fig. 14 Speed variation waveform under continuous disturbance

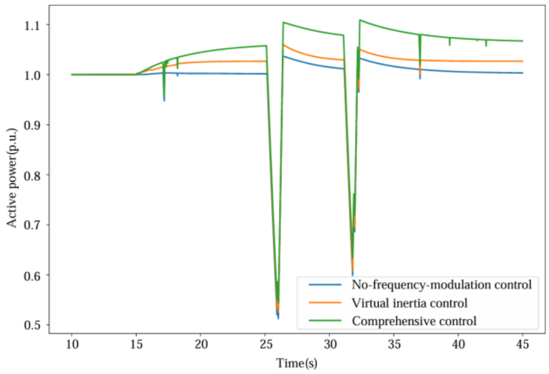

Fig. 15 Active power output variation waveform under continuous disturbance

It can be seen from Figure 13 that after the first load disturbance, the comprehensive control has the best effect on improving the lowest point of the system frequency; after the system suffers the second load disturbance, the virtual inertia control has a remarkable effect on increasing the lowest point of the system frequency. However, there is an obvious secondary drop at 32.46 s. As can be seen from Figures 14 and 15, the comprehensive control releases the most rotor kinetic energy and generates the maximum additional active power. Generally speaking, the comprehensive control proposed in this paper can respond quickly to frequency changes under continuous disturbances. The degree of frequency drop after the two disturbances has been significantly weakened, avoiding the secondary frequency drop. Moreover, the rotational speed shows a decreasing trend during the dynamic process of the frequency, releasing rotor kinetic energy, while rapidly increasing the active power generation, playing a good inertia support role.

4 Conclusions

This paper proposes a comprehensive regulation strategy that combines the variable coefficient virtual inertia control of doubly-fed wind turbines with primary frequency regulation, aiming to improve and optimize the primary frequency regulation control and virtual inertia control of doubly-fed wind turbines. The main conclusions are as follows:

(1) The virtual inertia control based on the dynamic power tracking proportional coefficient can avoid the impact caused by the step change of active power. Moreover, when the frequency drops significantly, it can quickly increase the electromagnetic power to provide frequency support, effectively improving the degree of frequency drop and enhancing the frequency stability of the power system.

(2) A comprehensive frequency regulation strategy that combines virtual inertia control and primary frequency regulation is proposed. This strategy enables the DFIG to quickly increase power generation for frequency support under any operating conditions, with a high response speed. It can also perform primary frequency regulation according to the static power-frequency characteristics of the unit, significantly improving the support of wind farms for system frequency. The simulation results show that the proposed frequency regulation coordination control strategy for wind farms can fully utilize the frequency regulation capability of wind farms and effectively support the power grid frequency.

References

[1] Li S, Fang T, Ye J. Damping to Low Frequency Oscillation Modes in DFIG-integrated Po wer System Based on Sensitivity to Controllable Loads[J]. Proceedings of the CSEE, 2024, 44(07): 2641-2655.

[2] Zhang x, Fu Y, Wang Y, et al. Integrated PSS Controller of Variable Speed Wind Turbine s with Virtual Inertia and Damping Control[J]. Transactions of China Electrotechnical Soci ety, 2015, 30(01): 159-169.

[3] Yao Y, Xiong Y, Yao W, et al. Adaptive Distributed Cooperative Control of Wind Farms for Grid Frequency Fast Support[J]. Proceedings of the CSEE, 2024, 44(02): 561-573.

[4] Li J, Gao Z, Li C, et al. Control Strategy for Dynamic Task Coefficient Based Primary F requency Regulation of Wind Power Assisted by Energy Storage[J]. Automation of Electri c Power Systems, 2021, 45(19): 52-59.

[5] MORREN J, DE HAAN S W H, KLING W L, et al. Wind turbines emulating inertia an d supporting primary frequency control[J]. IEEE Transactions on Power Systems, 2006, 21 (1): 433-434.

[6] Dong W, Zhang D, Cao Y, et al. The control strategies concerning the new type inertia fl ywheel and high-speed flywheel involved in the grid inertia response and primary frequen cy modulation[J/OL]. Energy Storage Science and Technology, 1-10[2024-12-03]. https://doi.org/10.19799/j.cnki.2095-4239.2024.0844.

[7] Van de Vyver J, De Kooning JD M, Meersman B, et al. Droop control as an alternative i nertial response strategy for the synthetic inertia on wind turbines[J]. lEEE Transactions o n Power Systems, 2015, 31(2): 1129-1138.

[8] Datta U, Shi J, Kalam A. Primary frequency control of a microgrid with integrated dyna mic sectional droop and fuzzy based pitch angle control[J]. International Journal of Electri cal Power and Energy Systems, 2019, 111248-259.

[9] Mehdi G, Gregor V, J. D H. Frequency Support From Wind Turbine Generators With a T ime-Variable Droop Characteristic[J]. IEEE Transactions on Sustainable Energy, 2018, 9(2): 676-684.

[10] Wang T, Cheng X. Variable droop coefficient control strategy of a DFIG considering rotor speed limit[J]. Power System Protection and Control, 2021, 49(9): 29-36.

[11] You R, Chai J, Sun X. Variable Speed Wind Turbine Micro-grid Frequency Regulation Co ntrol Based on Variable Droop[J]. Proceedings of the CSEE, 2016, 36(24): 6751-6758+692 9.

[12] Pan W, Quan R, Wang F. A Variable Droop Control Strategy for Doubly-fed Induction Ge nerators[J]. Automation of Electric Power Systems, 2015, 39(11): 126-131+186.

[13] Zhang F, Meng G, Sun Y, et al. Review on power system frequency modulation technolo gy under high permeability wind power grid connection[J]. Electrotechnical Application, 20 19, 38(09): 19-26.

[14] Ma K, Zhang L, Liu L. Primary Frequency Regulation Control of Wind Turbines in New Energy Power Systems Based on Consistency Algorithm[J]. Automation & Instrumentation, 2024, 39(05): 26-29+39.

[15] Wang Z, Zhang H. Research on Wind Energy Generation Technology and Power Control Strategy[J]. Process Automation Instrumentation, 2008, (11): 1-6.

[16] Liu H, Peng X, Zhang C, et al. Overview of wind power participating in frequency regul ation control strategy for power system[J]. Electric Power Automation Equipment, 2021, 4 1(11): 81-92.

[17] Wang T, Zhang F, Ding L. Frequency regulation control strategy of over-speed wind turbi nes considering optimal operation point[J]. Electric Power Automation Equipment, 2021, 4 1(06): 22-28.

[18] Cai G, Zhong C, Wu G, et al. Unit Commitment Strategy of Power System Considering Overspeed Load Reduction and lnertia Control of Wind Turbine[J]. Automation of Electric

Power Systems, 2021, 45(16): 134-142.
[19] Abouzeid I S, Guo Y, Zhang H, et al. Improvements in primary frequency regulation of t he grid-connected variable speed wind turbine[J]. IET Renewable Power Generation, 2019, 13(3): 491-499.
[20] Zhao X, Lin Z, Fu B, et al. Research on frequency control method for micro-grid with a hybrid approach of FFR-OPPT and pitch angle of wind turbine[J]. International Journal of Electrical Power & Energy Systems, 2021, 127: 106670.
[21] Prasad R, Padhy N P. Synergistic frequency regulation control mechanism for DFIG wind turbines with optimal pitch dynamics[J]. IEEE Transactions on Power Systems, 2020, 35 (4): 3181-3191.
[22] Zhang S, Dang J, Dai J, et al. Optimal Control Strategy for Wind Power Curtailment Con sidering Optimal Speed and Pitch Angle Control[J]. Power System Technology, 2021, 45(0 5): 1844-1851.
[23] Hei Y, Fu Y, Wang Y, et al. Selection of control parameters for wind power participating in frequency regulation and the analysis of its influence[J]. Electrical Measurement & Instr umentation, 2017, 54(05): 16-21+39.
[24] Ao B, Wang F, Chen L, et al. Primary Frequency Regulation Model and Aggregation of Deloading Wind Turbine Generators With Pitch Angle Adjustment[J]. Power System Techn ology, 2023, 47(04): 1360-1369.
[25] Zhang R, Li X, Gao Z, et al. Coordinated Control of Frequency-Regulation Reserve Capa city for Wind Farm Considering Wind Speed Difference[J]. Electric Power Construction, 2 023, 44(2): 101-109. https://doi.org/10.12204/j.issn.1000-7229.2023.02.010
[26] Ye H. Control technology of wind turbine generators[M]. Beijing: China Machine Press; 2 009: 144 - 149.
[27] Li H, Zhang X, Wang Y, et al. Virtual Inertia Control of DFIG-based Wind Turbines Bas ed on the Optimal Power Tracking[J]. Proceedings of the CSEE, 2012, 32(07): 32-39+188.
[28] He T, Sun L, Li S, et al. Research on Deloading Scheme and Primary Frequency Regulat ion Strategy of Wind Farm Considering Wind Speed Difference[J]. Electric Power Constru ction, 2022, 43(7): 139-148. https://doi.org/10.12204/j.issn.1000-7229.2022.07.016
[29] Fu Y, Wang Y, Zhang X, et al. Analysis and Integrated Control of Inertia and Primary Fr equency Regulation for Variable Speed Wind Turbines[J]. Proceedings of the CSEE, 2014, 34(27): 4706-4716.
[30] Ni Y. Theory and Analysis of Dynamic Power Systems[M]. Beijing: Tsinghua University Press; 2002.